Simulation of technologically relevant SPR devices

Author: Judith Costa Iracheta
Advisor: Mauricio Moreno Sereno
Facultat de Física, Universitat de Barcelona, Diagonal 645, 08028 Barcelona, Spain.*

Abstract: This work presents the simulation of the optical behavior of three different grating-based structures that can be used in the fabrication of Surface Plasmon Resonance (SPR) biosensors. For this, the OptiFDTD software package has been used. It has allowed to design the SPR sensors with different configurations and to adjust their technological parameters. Different values for the sensitivity have been obtained for the three structures and the differences have been explained.

I. INTRODUCTION

Surface plasmons (SP) are considered as quasiparticles resulting from the quantization of the propagating electron density waves occurring at the interface between a metal and a dielectric. Surface plasmons resonance (SPR) occurs when transverse magnetic (TM) p-polarized light (light polarized in the plane of the incidence) strikes the interface, interacting with the free electrons of the metal layer and causing a dip in the intensity of the reflected light. Since the oscillations are very sensitive to any change occurring at the interface, SPR devices are widely used as chemical and biological sensors.

II. SPR THEORY

For any interface between two media with different refractive indices, we can describe the complex reflection coefficient r_P for p-polarized incident light electric field, using Fresnel's equations:

$$r_P = \frac{E_r}{E_i} = |r_P|e^{i\varphi} = \left|\frac{tan(\theta - \theta')}{tan(\theta + \theta')}\right| e^{i\varphi} \qquad (1)$$

where E_i and E_r are the incident and the reflected electric fields, respectively, θ is the angle of incidence, θ' is the angle of refraction, and φ is a phase change of the reflected field respective to the incident field, which will rent depend on the materials involved.

From (1) it is seen that there are two main special cases: when $\theta + \theta' = \frac{\pi}{2}$, reflectance[1] tends to zero and there is no reflection for p-polarized light (this situation describes Brewster angle); the other case occurs when $\theta - \theta' = \frac{\pi}{2}$, reflectance tends to infinite, which means that the incident electric field is much smaller than the reflected electric field. This condition corresponds to resonance [1], which is the situation we want to work with. In this case, the dispersion relation is described as:

$$k_x = \frac{\omega}{c}\sqrt{\frac{\varepsilon_1\varepsilon_2}{\varepsilon_1 + \varepsilon_2}} \qquad k_{yi} = \frac{\omega}{c}\sqrt{\frac{\varepsilon_i^2}{\varepsilon_1 + \varepsilon_2}} \qquad (2)$$

where k_x and k_y are the components of the wavevector $\boldsymbol{k}$ of the light, ε_1 and ε_2 are the dielectric constants of materials 1 and 2, respectively, ω is the angular frequency of the propagated electromagnetic field, c is the velocity of light in vacuum, and i = 1 or 2.

Now, considering material 2 as a metal, containing many free electrons, we can define the dielectric constant as:

$$\varepsilon_2(\omega) = 1 - \frac{\omega_P^2}{\omega^2} \qquad (3)$$

where $\omega_P = \sqrt{4\pi n_e e^2/m_e}$ is known as *plasma frequency*, n_e is the free electron density, e is the elemental charge, and m_e is the electron mass.

For $\omega < \omega_P$, in equation (3), one obtains that the dielectric constant of the metal is negative and, therefore, no electromagnetic field can propagate in the metal. In fact, an electromagnetic wave exists, but it is only propagating along the interface, with evanescent tails perpendicular to it.

By substitution of (3) into (2), we can rewrite the surface plasmons dispersion relation as:

$$\omega^2 = (k_x c)^2 \cdot \left(1 + \frac{1}{1 - \left(\frac{\omega_P}{\omega}\right)^2}\right) \qquad (4)$$

which is represented in Fig.1.

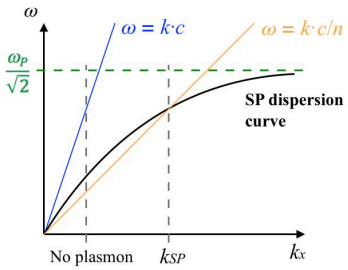

FIG. 1: Dispersion relation curve for surface plasmons (dark line). Blue and orange lines represent the dispersion relation for light in air (n=1) and in a material with refractive index n>1, respectively.

From Fig.1. it is seen that there is no intersection point between the dispersion relation for light in air (blue line) and the SP, which means that plasmons cannot be excited by light coming from air to the metal surface. Nevertheless, light coming from a material with refractive index greater than 1 (orange line) can cause SPR at the interface due to dispersion

[1] Reflectance is defined as $R_P = |r_P|^2$

* Electronic address: jcostair@gmail.com

relations lines crossing. From literature, it is known that this material should be a coupled prism [2]. Now, representing the reflectance of the emitted light in the interface between the material with n>1 and the metal as a function of the wavelength, we will find a dip due to the energy absorbed by the plasmons excitation (Fig.2).

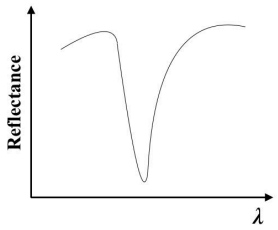

FIG. 2: SPR curve plotted in the representation of the reflected light as a function of the wavelength.

As per Fig.2, the wavelength at which the maximum loss of reflected light occurs is called resonant wavelength. This wavelength depends on the optical characteristics of the system, which in our case are the refractive indices at each side of the interface. If we experience a variation in the refractive index, e.g., due to an accumulated mass from aggregated proteins, the resonant wavelength will shift. This phenomenon will provide us information about the kinetics of protein adsorption on the surface. As a consequence, as indicated in the introduction, SPR devices are broadly operated as biological sensors.

SPR devices can be designed through different configurations, the three main ones being: Kretschmann configuration, in which surface plasmons are excited by a prism (structure described before); Otto configuration, in which plasmons are excited by an evanescent wave produced by total internal reflection; and grating configuration, in which the plasmon excitation is achieved using a diffraction grating [3].

In this work, we have simulated the grating configuration, where a metal layer with a periodic structure acts like a diffraction grating (see Fig.3), and when the incident light impinges the surface with a wavevector $k_x = 2\pi/\lambda n_i \sin\theta$, different diffraction orders m=0, ±1, ±2, … are generated in the reflected light. The corresponding wavevector can be written as:

$$k_{x,reflected} = k_x + m\frac{2\pi}{\Lambda} \qquad (5)$$

where Λ is the periodicity of the structure.

So, in this case, the diffracted waves can couple with a surface plasmon when their propagation constant and that of the surface plasmons are equal, which can be achieved by changing the incident angle of the incoming light.

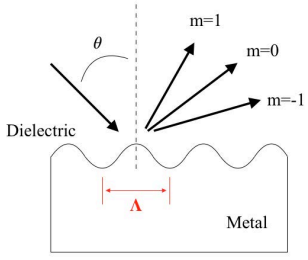

FIG. 3: Simplified sketch of a grating configuration for a SPR.

III. TECHNOLOGICAL ALTERNATIVES

The purpose of this work is to study different types of grating-based SPR devices and optimise the fabrication parameters to get the most sensitive response to refractive index variations.

We will introduce three different structures. The first two have been fabricated and will be measured in the future. The third one is a possible future device to be fabricated, which gives theoretical satisfactory results.

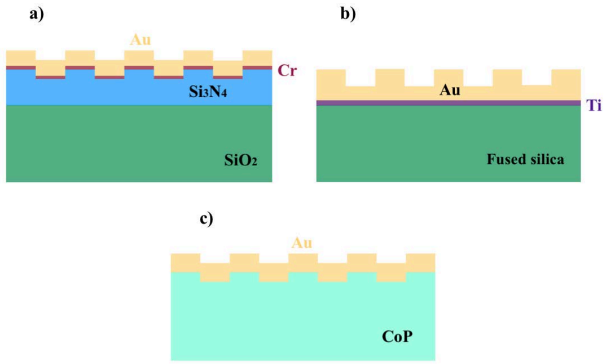

FIG. 4: Schematic representation of structures 1,2,3 under study.

A. Structure 1

The first structure consists of a Silicon substrate, oxidized to get a 1μm layer of SiO_2 above, and covered by a 100nm Si_3N_4 layer. In this case, diffraction grating has been obtained by etching the Si_3N_4 layer, followed by metal deposition, which we indicate as Au (in fact, this layer was a Cr/Au stack 5/45 nm, that assures the adhesion of Au), see Fig.4a. The grating had a semiperiod spacing ranging from 200 to 250nm and has been obtained using electron-beam lithography of a resist and reactive ion etching of the Si_3N_4.

B. Structure 2

This second structure consists of a fused silica substrate (n=1,445 [4]), covered by a Ti/Au stack. In this case, the etching was directly made in the gold layer, shown in Fig.4b. These gratings were fabricated using high energy laser interference lithography with a frequency tripled Nd:YAG nanosecond laser. The grating structures were first recorded in a photosensitive layer and afterwards transferred to a Au film.

C. Structure 3

This new structure is expected to be manufactured in the near future. It consists of flexible substrate made of cyclio-olefin polymer (COP) (n=1,53) and is shown in Fig.4c. We have chosen COP because it is an inexpensive material that cannot be dissolved by acetone and can be patterned using nanoimprint lithography, using hard stamps, like etched silicon substrates [5]. On top of it, a stack Ti/Au will be deposited.

IV. SIMULATOR

To design the structures to simulate, we used the software OptiFDTD 64-bitLayout Designer and Analyzer. It is based on the method FDTD (Finite-Difference Time-Domain), which solves Maxwell equations in a numerical grid [6].

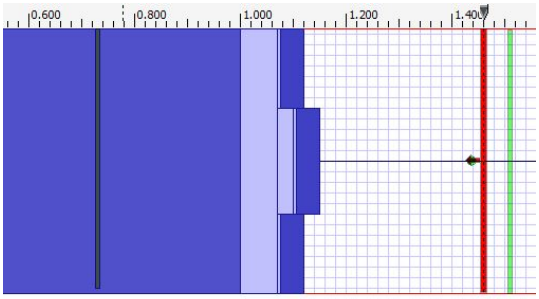

FIG. 5: OptiFDTD design of structure 1. From left to right we observe the SiO_2 layer (dark blue), followed by the Si_3N_4 coating (light blue), the Cr adhesion film (again light blue) and the final Au layer (dark blue). Red and green lines are the input and observation planes, respectively.

The structures designs are arranged in the x-z plane, with y-direction, perpendicular to the paper, assumed to be infinite. Propagation occurs along z direction, as explained in Fig.5. Then, incident wave properties are set: the time domain input plane chosen is a Gaussian modulated continuous wave. For the transverse field distribution, a rectangular transverse beam is selected. Also, we set periodic boundary conditions for x direction to represent an infinite surface for the structure.

All structures have been simulated with same 2D conditions: sampling mesh $\Delta x=0.005\mu m$, $\Delta z=0.005\mu m$.

Next, the modulated 2D TM Gaussian pulse is sent (red line in Fig.5.) to impinge the gold surface normal to it. This electromagnetic pulse has its central wavelength at 700nm. Then, the observation plane (green line in Fig.5) gets the information of the reflected light and the OptiFDTD Layout Analyzer is opened to show the results. It provides the reflection spectrum and it is time to analyse the outcomes.

V. RESULTS

In this section, we will focus on the results of the structures 1 and 2, which are selected in the interested of experimental measures, and we will give a general discussion of structure 3.

A. Structure 1

First, we would like to clarify that the only fixed parameter is the duty cycle (DC) of the tooth of the diffraction grating, which was 50% of the period. Gold thickness was 45 or 50nm, depending on the simulation. Then, we changed the periodicity of the grating, the etching depth and the external medium.

Fig.6 presents the simulated reflectance as a function of the incident wavelengths. As we can see, the resonant wavelength moves towards the infrared both as a function of the period of the grating and the refractive index of the external medium.

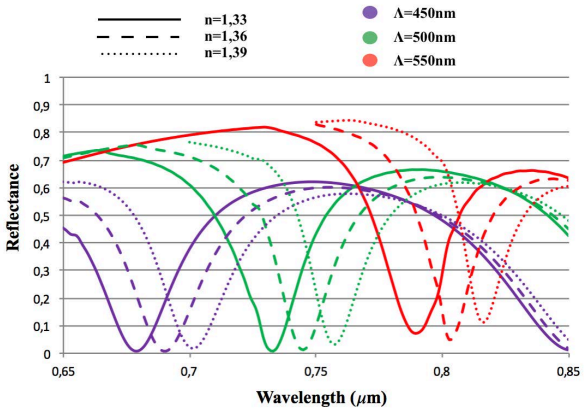

FIG. 6: Resonant reflectance of structure 1 for a gold layer of 45nm, etching depth of 40nm, DC=50%, periods of the grating of 450, 500 and 550nm and external media with n=1.33, 1.36 and 1.39.

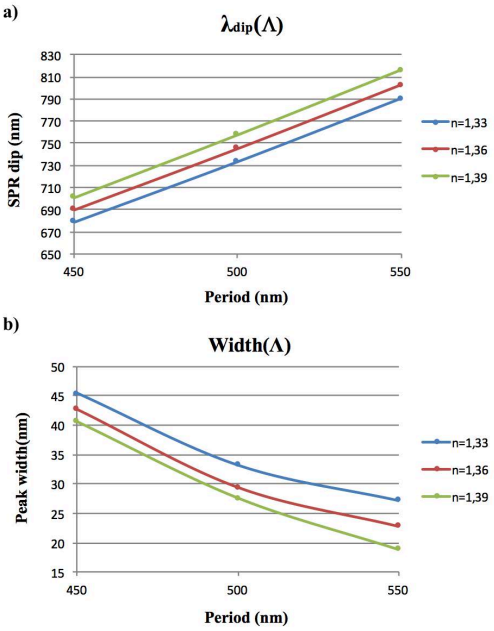

FIG. 7: SPR wavelength dip (a) and peak width (b) of structure 1 as a function of the periodicity of the grating for a gold layer of 50nm, etching of 40nm, DC=50%, and external media with n=1.33, 1.36 and 1.39.

From Fig.7. we confirm that, increasing the periodicity of the grating, on the one hand, the resonant wavelength shifts towards the infrared, and on the other, the width of the resonance peaks becomes narrower.

One of the most searched parameters in SPR-based biosensors is sensitivity, which is the relation between the variation of the resonant wavelength and the variation of the external medium refractive index. It is represented in Fig.8. for structure 1.

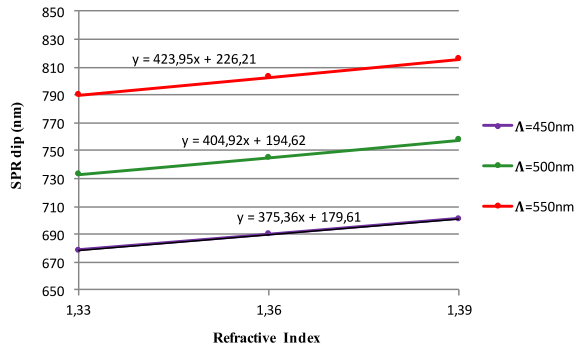

FIG. 8: Sensitivity of the SPR sensor of structure 1 for different periodicities of the grating.

As seen in Fig.8, the sensor sensitivity increases with the grating period. For a period of 550nm, the sensitivity is almost 424nm.

From Fig.6. it can easily be seen that, looking at the period of 450nm, a second resonant peak appears shifted about 150nm to the higher wavelengths. This was an unexpected result because this second peak did not appear in the preliminary experimental measurements. For this reason, we modified the simulated structure to include the chromium adhesion layer to see whether it affected the result or not.

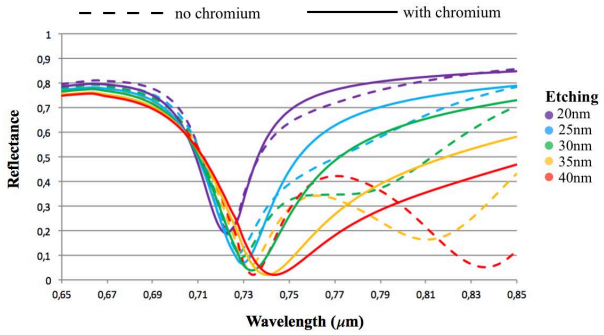

FIG. 9: Resonant reflectance for structure 1, with and without chromium adhesion layer, for different etchings. Λ=500nm, DC=50%, n(external medium)=1.33, gold layer of 45nm (with Cr=5nm) or 50nm (without Cr).

As is clear (see Fig. 9), the effect of the adhesion layer is relevant in the reflectance results, giving rise to a reduction of the intensity of the second peak. It is known, that Cr and Ti have high absorption properties in the optical region, which considerably influences the optical transmission of the structure [7].

B. Structure 2

For this structure, and from previous simulations, we found that the best parameters to use (in SPR sensors we want to obtain resonant peaks as narrow and deep as possible) were: 50nm of Au, 30nm of etching depth, and 50% of duty cycle.

Now, we wanted to know if the adhesion layer did also affect our results. Prove of that is Fig.10., which shows that, as it happened for structure 1, the intensity of the second peak is strongly reduced.

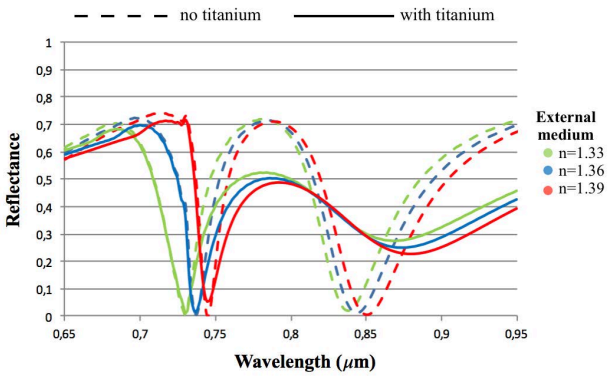

FIG. 10: Resonant reflectance for structure 2, with and without titanium adhesion layer, for different external media. Λ=500nm, DC=50%, 30nm of etching depth, gold layer of 45nm (with Ti=5nm) or 50nm (without Ti).

Here we will use similar figures as for structure 1, so that we can discuss the observed differences. In Fig.11 it is seen that, again, increasing the periodicity of the grating shifts the resonant wavelength towards the infrared for any external medium. However, in this case, peak width as a function of the period is not as linear as for structure 1 and some of the peaks of longer periods are wider than expected. This is the result of considering the adhesion layer in these next simulations, something we did not do in structure 1.

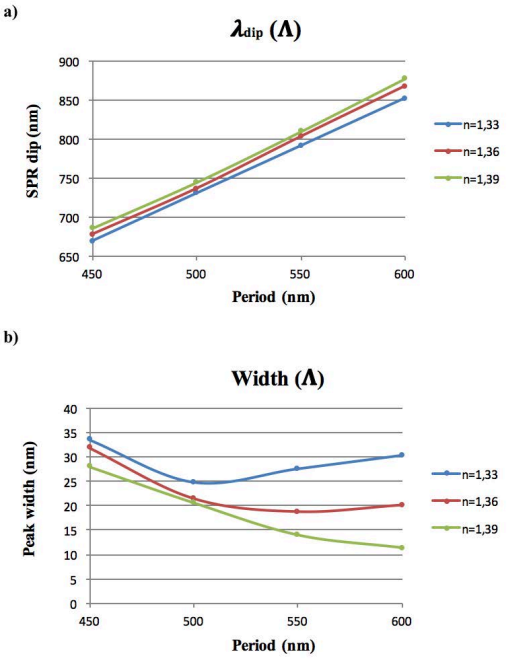

FIG. 11: Representation of SPR wavelength dip(a) and peak width(b) for structure 2 as a function of the periodicity of the grating for a gold layer of 45nm, plus the 5nm titanium adhesion layer, etching=30nm, DC=50%, and external mediums with n=1.33, 1.36, 1.39.

Finally, we found that the sensitivity of structure 2 (see table I), like in the previous case, highest maximum at the largest grating period. Also, from these simulations, we conclude that structure 1 has better sensitivity than structure 2 for the same period (here, at 550nm at table I, sensitivities are 424nm and 312 for structures 1 and 2, respectively).

C. Structure 3

In structure 3, we performed similar simulations as for structures 1 and 2. We varied five parameters: etching depth, periodicity and duty cycle of the grating, external medium, and gold thickness. In brief, we confirm that short etchings or small DCs result in shallow peaks, and long etchings or large DCs result in peaks too wide. Again, that increasing periodicity, peaks become narrower, and gold thickness=100nm gives better sensitivity.

In summary, the better parameters to work with for this structure were: etching=30nm, DC=50%, period=600nm, gold thickness=100nm.

D. Comparison among the structures

Finally, the table comparing the sensitivity of each structure is shown here.

	1	2	3	
			Gold=50	Gold=100
Λ=450nm	375	280	-	-
Λ=500nm	405	243	474	512
Λ=550nm	424	312	548	571
Λ=600nm	-	425	617	627

TABLE I: Sensitivity (in nm) of structures 1,2,3, shown for different periodicities of the gratings.

As it is seen, the structure with highest sensitivity is the one made of COP, covered by a 100nm gold layer and with a grating periodicity of 600nm, which gives an approximate value of 627nm.

VI. CONCLUSIONS

- Our simulations get resonant dips in reflected light sharp and narrow, which match the experimental values in literature.
- SPR resonant wavelength shifts towards the infrared when increasing periodicity of the grating.
- The (necessary) adhesion layer affects the results by reducing the second observed peak and by increasing the peak's width.
- Structures 1 and 3, geometrically similar, have better sensitivities than structure 2, apparently, because their pseudosubstrates follow the surface structure. On the other hand, between 1 and 3, we observe higher sensitivity for the latter, probably because COP has a lower refractive index than Si_3N_4.
- Sensitivity is enhanced by increasing the periodicity of the grating.
- Structure 3 gives theoretical satisfactory results and, simultaneously, its fabrication is cost-effective, making it a future promising SPR device.
- This work has allowed me to apply some of my previous theoretical knowledge, gained during the bachelor, to a technologically relevant problem.

Acknowledgments

I would like to thank my advisor, Dr. Mauricio Moreno, for his patience and his long tutoring work. I would also want to thank Dr. Albert Romano, for believing in me and for his willingness to help and teach. Lastly, I would not finish my acknowledgements without mentioning my family and friends, who showed unconditional support during this years, and helped to make this work come true.

[1] R.B.M. Schasfoort and A.J. Tudos, «Handbook of Surface Plasmon Resonance», Royal Society of Chemistry, RSC Publishing. ISBN: 9780-85404-267-8., 2008.

[2] «Springer Series on Chemical Sensors and Biosensors», Series Editor: O.S. Wolfbeis, ISBN-13: 978-3540339182, 2006.

[3] P.Rodríguez, «Design and functionalization of optical resonant structures for biological applications», Final project on Master of Biophysics, 2010/11.

[4] L.H. Malitson, «Interspecimen Comparison of the Refractive Index of Fused Silica», *Journal of the Optical Society of America*, vol. 55, issue 10, p.1205, October 1965.

[5] S. Kumari, S. Mohapatra and R.S. Moirangthem, «Development of flexible plasmonic plastic sensor using nanograting texture laminating film», Mater. REs. Express 4 (2017) 025008.

[6] R. Umeda, C. Totsuji, K. Tsuruta and H. Totsuji, «Dispersion Models and Electromagnetic FDTD Analyses of Nanostructured Metamaterials using Parallel Computer», *Memoirs of the Faculty of Engineering*, Okayama University, vol.43, pp.8-15, January 2009.

[7] M. Najiminaini, F. Vasefi, B. Kaminska, J.J.L. Carson, «Optical resonance transmission properties of nano-hole arrays in a gold film: effect of adhesion layer», *Optics Express*, vol.19, issue 27, pp. 26186-26197, 2011.